Lawrence F. Torkan
Centre for Health Innovation,
Queen's University,
Kingston, ON M5B0B7, Canada;
Department of Mechanical and
Materials Engineering,
Queen's University,
Kingston, ON M5B0B7, Canada

John T. Bryant
Centre for Health Innovation,
Queen's University,
Kingston, ON K7L3N6, Canada;
Department of Mechanical and
Materials Engineering,
Queen's University,
Kingston, ON K7L3N6, Canada

Ryan T. Bicknell
Centre for Health Innovation,
Queen's University,
Kingston, ON K7L2V7, Canada;
Department of Surgery,
Queen's University,
Kingston, ON K7L2V7, Canada

Heidi-Lynn Ploeg
Centre for Health Innovation,
Queen's University,
Kingston, ON K7L3N6, Canada;
Department of Mechanical and Materials
Engineering,
Queen's University,
Kingston, ON K7L3N6, Canada

Accuracy of an Apparatus for Measuring Glenoid Baseplate Micromotion in Reverse Shoulder Arthroplasty

Reverse shoulder arthroplasty (RSA) is used to treat patients with cuff tear arthropathy. Loosening remains to be one of the principal modes of implant failure and the main complication leading to revision. Excess micromotion contributes to glenoid loosening. This study sought to determine the predictive accuracy of an experimental system designed to assess factors contributing to RSA glenoid baseplate micromotion. A half-fractional factorial experiment was designed to assess 4 factors: central element type (screw versus peg), central element length (13.5 versus 23.5 mm), anterior-posterior peripheral screw type (locking versus nonlocking) and cancellous bone density (10 versus 25 pounds per cubic foot (pcf)). Four linear variable differential transducers (LVDTs) recorded micromotion from a stainless-steel disk surrounding a modified glenosphere. The displacements were used to interpolate micromotion at each peripheral screw position. The mean absolute percentage error (MAPE) was used to determine the predictive accuracy and error range of the system. The MAPE for each condition ranged from 6.8% to 12.9% for an overall MAPE of (9.5 ± 0.9)%. The system had an error range of 2.7 μm to 20.1 μm, which was lower than those reported by prior studies using optical systems. One of the eight conditions had micromotion that exceeded 150 μm. These findings support the use of displacement transducers, specifically LVDTs, as an accurate system for determining RSA baseplate micromotion in rigid polyurethane foam bone surrogates.
[DOI: 10.1115/1.4055063]

Introduction

Reverse shoulder arthroplasty (RSA) is typically performed to treat patients with rotator cuff arthropathy, osteoarthritis (OA), and complex proximal humerus fractures [1–5]. RSA systems involve a reversal of the native ball-and-socket aspects of the glenohumeral joint. Implant designs typically consist of a polyethylene humeral cup affixed to a stem placed within the proximal humerus and a glenosphere secured to a baseplate implanted on the glenoid fossa of the scapula. Baseplates may be centrally secured by means of a press fit peg or a central compression screw. Although it has a relatively high rate of complications, RSA has been shown to be effective in improving patient functional outcomes, pain, and quality of life [6–8].

One of the most common complications in RSA is glenoid baseplate loosening, which will often require revision surgery [9–11]. Given the increase in the volume of primary RSA, a comprehensive understanding of the baseplate features that affect baseplate loosening is of critical importance to prevent or delay revision of the glenoid component [12]. RSA implants allow for enhanced long-term fixation by inclusion of a hydroxyapatite coating. For the interface bone to effectively mineralize onto the hydroxyapatite-coated implant, micromotion of the baseplate with respect to the interface surface should be limited to a range of 50 μm to 150 μm [13–17]. Implant-related factors that may affect fixation of the baseplate to the glenoid, and thus, micromotion, include the patient's bone quality, peripheral screw properties, and the central fixation element. The literature regarding these factors is limited, as are reports of long-term outcomes. Therefore, it is essential that the mechanically testing of RSA implant micromotion be conducted with reliable measurement systems.

Implant micromotion is defined as implant displacement relative to the site of bone resection while under cyclic loading, and has been measured and modeled in a variety of ways. Some studies have employed computer-generated models to simulate mechanical loading of baseplates by means of finite element analysis [18–20]. Others have tested baseplate fixation using cadavers or polyurethane (PU) foam bone surrogates [1,18,21–30]. The rationale for the use of PU foam instead of cadaveric material is threefold: (1) to reduce variability in experimental measures; (2) to reduce costs, thus simplifying procurement; and (3) to avoid using biohazardous materials [18]. Bone-implant micromotion has been measured using various devices, such as displacement transducers (e.g., linear variable differential transformers (LVDTs), differential variable reluctance transducers) and three-dimensional (3D) motion capture systems [18,21,22,25,27]. Digital image correlation or digital volume correlation with microcomputed tomography (CT) may also be used in micromotion analyses [31,32].

Several studies have reported the results of the mechanical testing of micromotion, but few have reported the accuracy of the apparatuses. A study by Göpfert et al., using a 3D video-based system, found that the accuracy of their system (reported as 36 μm) was dependent on the number of cameras tracking the reflective markers [33]. Another study found that the distance between the camera systems and the rigid body, as well as the tilt angle of the rigid body, affected the accuracy of such measurements (< 30 μm reported in this study) [31,34].

The present work involved an experiment designed to evaluate factors that affect micromotion of the Delta XTEND™ Reverse

Manuscript received October 27, 2021; final manuscript received July 19, 2022; published online August 5, 2022. Assoc. Editor: Nandini Duraiswamy.

Shoulder System (De-Puy Synthes, Warsaw, IN), specifically, the effects of the method of central element fixation, level of cortical engagement, peripheral screw configuration, and varying cancellous bone densities. The purpose of this study was, therefore, to determine the predictive accuracy of the LVDT system that captured baseplate micromotion measurements relative to the bone surrogate in this experiment. Accuracies were expected to closely resemble the results of a preliminary pilot experiment (N = 6), which employed a similar methodology, reporting an error of (6.0 ± 1.2)%.

Materials and Methods

This study measured the micromotion of the Delta XTEND™ glenoid baseplate relative to a bone surrogate under a combined compressive and shear load. In this study, micromotion was defined as the displacement range of the glenoid baseplate relative to the bone surrogate in the medial-lateral (*Z*) direction (see axes Fig. 1). The factors investigated were central element fixation (i.e., press-fit peg or compression screw), cortical engagement of longer central elements with 30 pounds per cubic foot (pcf) cortical density PU foam (i.e., 13.5 and 23.5 mm), anterior-posterior (A-P) peripheral screw-type (i.e., locking or nonlocking), and cancellous bone density (i.e., 10 pcf and 25 pcf).

The glenoid bone was physically modeled with a custom-made, laminated bone surrogate constructed from Sawbones™ rigid PU foam blocks (Pacific Research Laboratories, Vashon Island, WA) with cancellous densities of 10 pcf (osteoporotic) or 25 pcf (healthy), and a 30 pcf cortical density. Each sample consisted of a 16 mm-thick cancellous layer (10 or 25 pcf), to simulate scapular bone stock, laminated over a 134 mm-thick cortical density PU foam block (30 pcf), with final dimensions of 40 mm × 40 mm × 150 mm. The thickness of the cancellous layer (16 mm thick) was chosen to prevent deep engagement of short central fixation elements (13.5 mm long) with the cortical density foam. Central screw baseplates were modified by removing the peg of an original baseplate and milling a countersunk hole, in order to accommodate a 6.5 mm diameter central cancellous screw (Product #218.030, De-Puy Synthes).

Experimental Design. This experiment was designed as a half-fractional factorial (2^{k-1}) to omit factor combinations that were specifically relevant to higher order interactions. The design involved four factors (k = 4) at two levels each. The experiment, therefore, had eight unique factor conditions, each of which was repeated five times for a total of 40 runs (N = 40). The eight conditions were as follows: (1) 13.5 mm central peg with nonlocking A-P screws in 10 pcf PU foam; (2) 13.5 mm central screw with nonlocking A-P screws in 25 pcf PU foam; (3) 23.5 mm central peg with nonlocking A-P screws in 25 pcf PU foam; (4) 23.5 mm central screw with nonlocking A-P screws in 10 pcf PU foam; (5) 13.5 mm central peg with locking A-P screws in 25 pcf PU foam; (6) 13.5 mm central screw with locking A-P screws in 10 pcf PU foam; (7) 23.5 mm central peg with locking A-P screws in 10 pcf PU foam; and, (8) 23.5 mm central screw with locking A-P screws in 25 pcf PU foam (Table 1, Fig. 2).

Each sample was cyclically loaded in an inferior-to-superior and lateral-to-medial direction at 60 degrees to the loading platform, with a load range of 500 N (20 N to 520 N; 1 Hz). This loading protocol simulated peak loading experienced during shoulder abduction while performing activities of daily living (e.g., brushing one's hair) during the first three postoperative months, which are most vital for initial osseointegration [35,36]. The load was force-controlled and applied using a materials testing system (Bionix Servohydraulic Test System; MTS Systems Corporation,

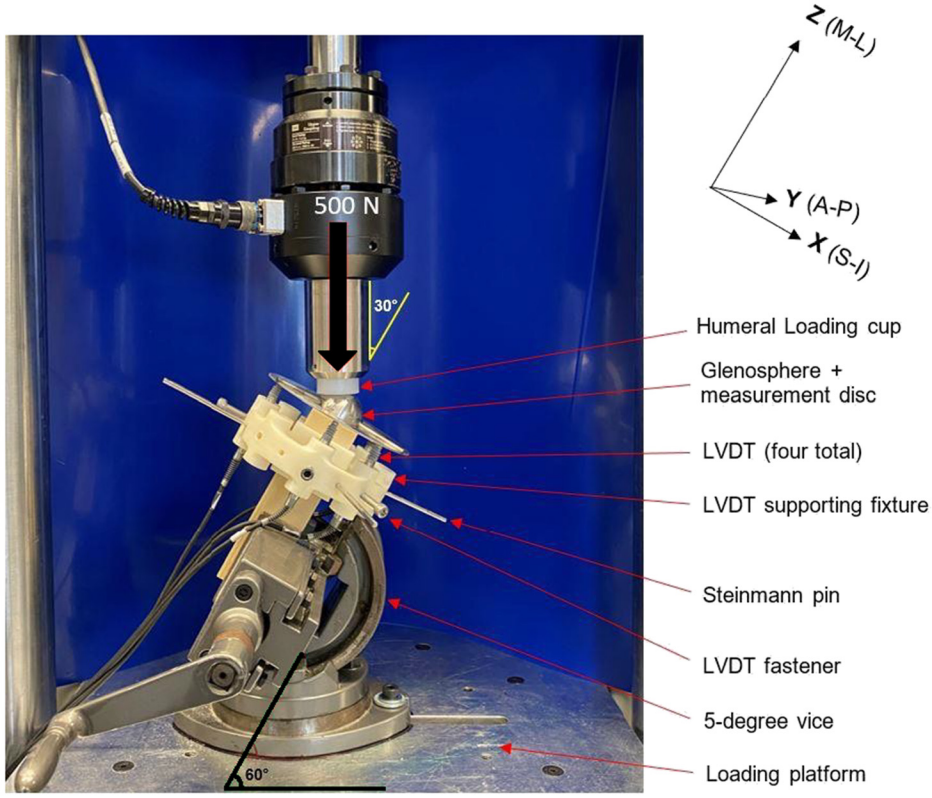

Fig. 1 The experimental configuration used for each run with the labels for the modified glenosphere and LVDT is highlighted in bold. Samples were secured at 60 deg to the loading platform. Implants were cyclically loaded with 500 N maximum and 20 N minimum sinusoidal load at 1 Hz for 1000 cycles. The *X*-, *Y*-, and *Z*-axes represent the superior-inferior (S-I), anterior-posterior (A-P), and medial-lateral (M-L) directions, respectively.

Table 1 The half-fractional factorial experiment shows the eight unique factor conditions

Condition	A	B	C	D=ABC
1	−	−	−	−
2	+	−	−	+
3	−	+	−	+
4	+	+	−	−
5	−	−	+	+
6	+	−	+	−
7	−	+	+	−
8	+	+	+	+

Factor	−	+
A: Central fixation	Peg	Screw
B: Central length	13.5 mm	23.5 mm
C: A-P Screw type	Nonlocking	Locking
D: Cancellous density	10 pcf	25 pcf

Eden Prairie, MN); axial force and displacement across time were collected using a load cell (5 kN capacity), and the loading frame crosshead, respectively, at a sampling rate of 20 Hz. Each sample was first loaded with 20 N, tared, then loaded cyclically for 1000 sinusoidal cycles. Baseplate displacement was recorded on a laptop by four LVDTs at a sampling rate of 20 Hz.

Micromotion Apparatus. The apparatus consisted of an angled 5-degree-of-freedom vice, a custom-made LVDT support fixture, the baseplate implanted within the PU foam block, a modified glenosphere with a measuring disk, and a humeral loading cup (Fig. 1). The glenosphere was connected via three, welded spokes to a circular stainless-steel disk from which displacement measurements were recorded. Baseplates were implanted at the center of the top face of each PU foam block. The measurement disk served to expand the area of the implant plane, thus allowing four LVDT probes (Orbit 3, Solartron^{TM} Metrology, West Sussex, UK) to record the displacement of the implant relative to the bone surrogate. The 5-degree-of-freedom vice positioned the sample at 60 deg to the loading platform such that compressive loading occurred at 30 deg to the implant axis (*Z*-axis, M-L), a configuration identical to that of previous micromotion experiments [22].

The LVDTs had a resolution of 3 μm and a measuring range of 2000 μm. Each LVDT was fastened within a custom-made support fixture (3D-printed with acronitryl butadiene styrene) affixed to each PU foam block. The fixture included a 40 mm × 40 mm central square through hole to ensure that the radial distance of each LVDT from the center was repeatable sample-to-sample. Displacement was measured in the medial-lateral direction, represented by the *Z*-axis (Fig. 1). Each LVDT was located at a radius of 52.5 mm from the center of the baseplate at 0 deg, 135 deg, 225 deg, and 270 deg, with respect to the position of the inferior peripheral screw (Fig. 3). Displacement data were collected during the last 10 cycles of the loading phase, as well as at the beginning and end of the cycle without any loading. Differences between the latter two values were used to calibrate the measurements, thus accounting for any possible migration of the implant.

Measurement Accuracy. The *X-Y* position for each LVDT was determined using their radii and angular positioning within the supporting fixture (Fig. 4). Measured displacements in the *Z*-direction were used to determine the *Z*-coordinate of the measurement disk where it made contact with the LVDT probe with respect to the supporting fixture. Micromotion in the *Z*-direction was determined by subtracting the minimum displacement (i.e., the reference) from the maximum displacement (*zLVDTi* – *zLVDTi* reference) for each LVDT obtained during the loading phase. The *X-Y* positions of LVDTs #1, #2 and #3 determine the values of two vectors, *L1* and *L2*. The cross-product of these two vectors defined the plane of the supporting fixture (and the parallel measurement disk) with planar coefficients *a*, *b*, *c*, and *d*. Once the equation of the plane was established, the position of LVDT #4 was substituted into the equation of the plane to determine its predicted displacement in the *Z*-direction. Finally, the measured and predicted displacement values were compared to quantify the accuracy of the micromotion measurements. Micromotion at each respective screw position (inferior, anterior, superior, posterior) was interpolated using the equation of the plane and the displacement data captured by each LVDT. The difference between the predicted and measured micromotion values at LVDT #4 for each sample at the corresponding screw position (i.e., anterior) was averaged and used to compute the mean absolute percentage error (MAPE) of the system, respective of condition. The MAPE for each condition was found using Eq. (1):

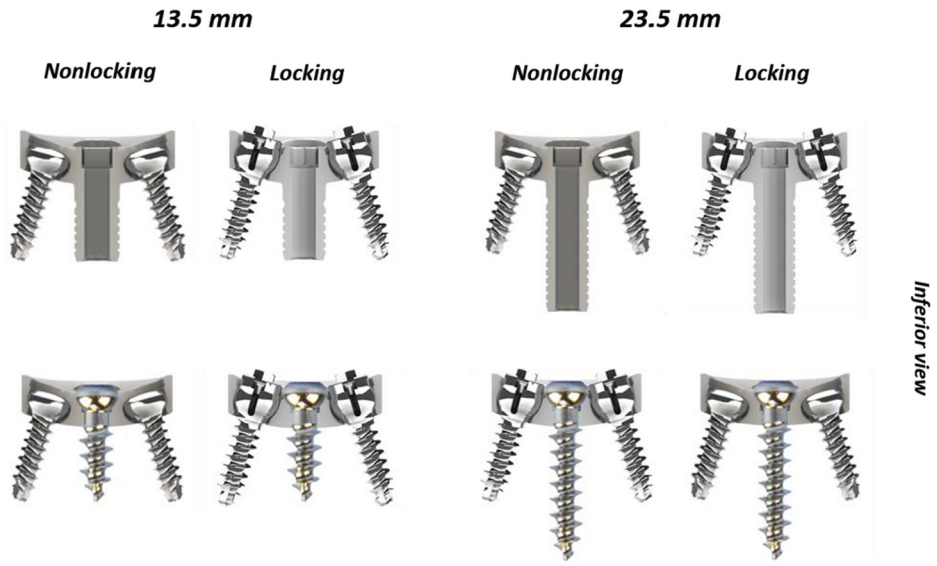

Fig. 2 Section views (transverse plane with respect to anatomical position) of each of the eight unique factor combinations: central element length, nonlocking versus locking, and central peg versus screw. Long central elements (23.5 mm) engaged with higher density PU foam at cortical depths.

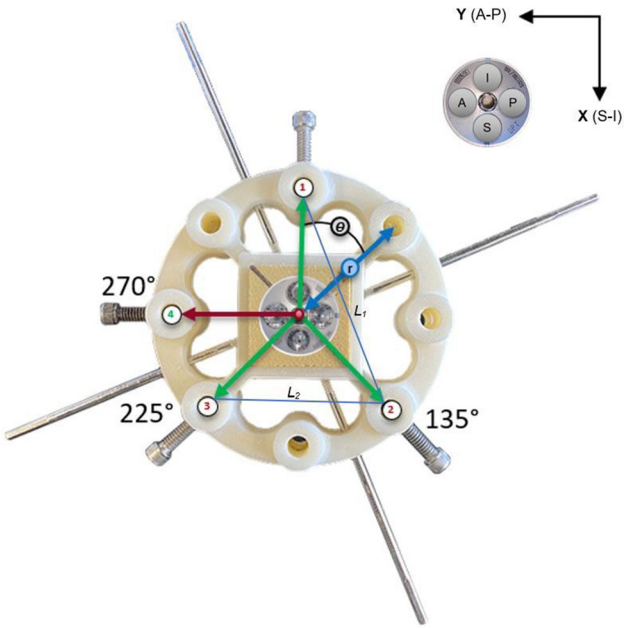

Fig. 3 The positions of each LVDT in the supporting fixture (circled numbers). Lines labelled *L1* and *L2* were vectors connecting LVDT #1 and #2, and #2 and #3, respectively. The position of LVDT #4, indicated at 270 deg from LVDT #1, served as the reference position to be compared to the predicted displacement at the anterior screw position. The inset at the top right shows four screw positions: inferior (I), medial (M), superior (S), and anterior (A).

$$\text{mean absolute percentage error (MAPE)} = \frac{1}{n}\sum \left| \frac{(z_4)_{\text{measured}} - (z_4)_{\text{predicted}}}{(z_4)_{\text{measured}}} \right| \quad (1)$$

where n was the number of conditional repeats, $(z_4)_{\text{measured}}$ is the measured displacement in the Z-direction at LVDT #4, and $(z_4)_{\text{predicted}}$ is the predicted displacement in the Z-direction at the anterior screw position.

Results

The mean absolute percentage error for each condition ranged from 6.8% to 12.9% for an average MAPE of (9.5 ± 0.9)% (Table 2). An example of the micromotion data recorded by LVDTs #1 to #4 for a sample with a combination of a 23.5 mm central peg, locking A-P screws, and 10 pcf cancellous bone can be seen in Fig. 5. This shows the cyclic displacement of the implant relative to the bone surrogate during loading. The peak micromotion, 39 μm, was recorded by LVDT #2, and peaks for LVDTs #1 to #3 ranged from 32 μm to 34 μm. The peaks varied slightly due to the tilting of the baseplate and the relative positions of the LVDTs. Tilting of the baseplate was confirmed by the plane for each sample, which indicated that the plane of displacement was not orthogonal to the Z-direction.

Discussion

The long-term success of RSA relies partly on the primary fixation of the glenoid baseplate to the interface bone. Reliable and accurate micromotion test methods are therefore required to draw clinically relevant conclusions regarding optimal baseplate factors, such as the implant design and positioning, peripheral screw configuration, or patient bone quality. This is also of importance to computer-assisted modeling studies that use such experimental data as a standard for validation [32]. Therefore, this study evaluated the predictive accuracy of a measurement system designed to test factors that affect glenoid baseplate micromotion in vitro, specifically, the effects of central element type, central cortical engagement, peripheral locking screw configuration, and bone density. Loading in this experiment was limited to 1000 cycles, given that a cycle count that exceeds 1000 does not provide additional information related to primary fixation [24]. Micromotion was measured using a displacement transducer system consisting of four LVDTs.

Previous studies have used a variety of measurement systems for measuring glenoid baseplate micromotion, however, the accuracies of these systems have gone relatively undocumented. The analysis of this study yielded a MAPE range of 6.8% to 12.9%, an error range of 2.7 μm to 20.1 μm, and an overall MAPE of (9.5 ± 0.9)%. The error range was lower than those reported by studies using optical systems, indicating enhanced precision [33,34]. These results are similar to the findings of a related pilot experiment conducted at our center, in which a MAPE of (6.0 ± 1.2)% was measured. The present study included more

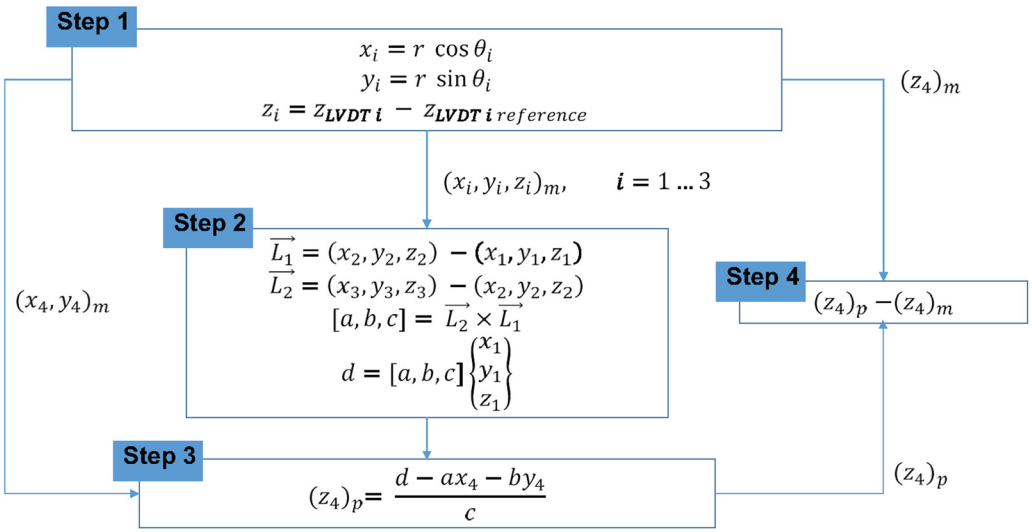

Fig. 4 The four-step algorithm is used to compute the predicted displacement of a given LVDT in the *Z*-direction. The micromotion, *zi*, was found by subtracting the maximum displacement of a given LVDT, *zLVDTi*, from its minimum displacement, *zLVDTi* reference.

Table 2 Micromotion averaged from each screw position and the associated MAPE for each condition with average MAPE and standard error

Condition	Inferior (μm)	Anterior (μm)	Superior (μm)	Posterior (μm)	Average (μm)	MAPE (%)	Error (μm)
(1) Peg/13.5 mm/NL/10 pcf	316.8	310.5	273.7	280.0	295.2	6.8	20.1
(2) Screw/13.5 mm/NL/25pcf	38.8	39.5	39.5	38.8	39.2	12.9	5.0
(3) Peg/23.5 mm/NL/25pcf	43.8	46.0	49.3	47.1	46.6	8.3	3.9
(4) Screw/23.5 mm/NL/10pcf	16.0	20.0	30.4	26.4	23.2	11.7	2.7
(5) Peg/13.5 mm/LK/25pcf	146.3	137.1	130.6	91.4	137.9	6.9	9.5
(6) Screw/13.5 mm/LK/10pcf	42.5	44.8	52.0	49.7	47.3	8.8	4.2
(7) Peg/23.5 mm/LK/10pcf	44.0	43.7	40.0	40.2	42.0	7.9	3.3
(8) Screw/23.5 mm/LK/25pcf	23.2	23.4	22.7	22.5	23.0	12.9	3.0
					Average	9.5	6.5
					St. Error	0.9	2.1

combinations of factors and a larger sample size than the pilot experiment, however, both experiments yielded similar and promising results regarding the predictive accuracy of such measurement systems.

The average micromotion observed for each condition varied with respect to the optimal osseointegration range (50 μm to 150 μm). The micromotion measurement error range (2.7 μm to 20.1 μm) was significantly lower than the measured micromotion. The average micromotion for condition 6 (137.9 μm, error 4.2 μm), which was tested in 25 pcf PU bone, remained within the osseointegration range, and conditions 3 and 5, which involved 25 pcf and 10 pcf PU bone, respectively, had average micromotion values that approached the lower limit of 50 μm (46.6 μm and 47.3 μm; error range: 3.9–9.5 μm, respectively). Conditions 2, 4, 7, and 8 fell well below the lower threshold (39.2 μm, 23.2 μm, 42.0 μm, and 23.0 μm, respectively; error range: 2.7–5.0 μm). Condition 1 exceeded the upper limit of the threshold (295.2 μm; error: 20.1 μm), indicating a lower primary fixation compared to the other conditions. These results suggest that the micromotion measurements were accurate enough to differentiate between factor combinations. For example, a long central peg and nonlocking A-P screws (condition 4; error: 2.4 μm), or a short central peg with locking A-P screws (condition 4; error: 9.5 μm), may be well-suited for implantation within nominally healthy bone. Furthermore, a short central screw with locking A-P screws (condition 6; error: 4.2 μm) may provide adequate levels of fixation when implanted in osteoporotic bone.

Prior groups have acknowledged the limitation of displacement transducers given that, in most cases, micromotion can only be quantified in a single axis [37–40], as was the case for this study. The present experiment was limited in that only one measurement system was used (LVDTs), measuring micromotion in one axis, and that baseplate micromotion was modeled in a synthetic PU foam bone surrogate. Furthermore, the PU bone surrogates experienced a slight deflection during loading (bending in the direction of loading); however, since the LVDTs were directly mounted onto each sample, the system was able to measure the micromotion of the implant relative to the bone surrogate without significant interference from the material's deflection. An evaluation of identical factors using cadaveric specimens and/or finite element analysis could potentially corroborate the micromotion results of the present work and validate the accuracy of the apparatus. Additionally, use of digital image correlation, or digital volume correlation with CT, may be a potential avenue for overcoming the limitations of displacement transducers in micromotion analyses [32,41].

The findings presented here support the use of displacement transducers, specifically LVDTs, as an accurate system for determining RSA baseplate micromotion in a rigid PU foam bone surrogate. Future work investigating additional factors that affect the

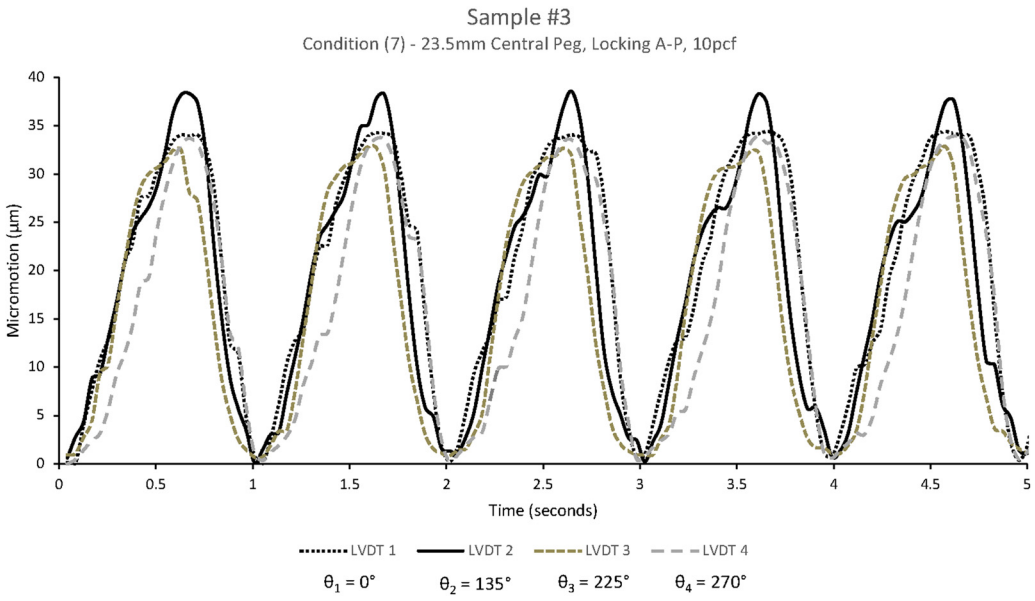

Fig. 5 Displacement data showing five cycles for sample #3 (23.5 mm central peg, locking A-P screws, 10 pcf cancellous bone). A peak displacement of 39 μm was recorded by LVDT #2.

accuracy of baseplate micromotion using various models could expand upon and validate the present results.

Conflict of Interest

Financial support was provided by Queen's University Faculty of Engineering and Applied Science. We acknowledge the support of the National Sciences and Engineering Research Council of Canada (NSERC; le Conseil derecherches en sciences naturelles et en génie du Canada; CRSNG) and additional research support from the Kingston Health Sciences Center, De-Puy Synthes, Zimmer Biomet, and ConMed Linvatec. The author RTB is a paid consultant for De-Puy Synthes and Zimmer Biomet. The other authors, their immediate families, and any research foundation with which they are affiliated have not received any financial payments or other benefits from any commercial entity related to the subject of this article.

References

[1] Chebli, C., Huber, P., Watling, J., Bertelsen, A., Bicknell, T., and Matsen, F., 3rd., 2008, "Factors Affecting Fixation of the Glenoid Component of a Reverse Total Shoulder Prothesis," J. Shoulder Elbow Surg., **17**(2), pp. 323–327.
[2] DiStefano, J. G., Park, A. Y., Nguyen, T. Q., Diederichs, G., Buckley, J. M., and Montgomery, W. H., 3rd., 2011, "Optimal Screw Placement for Base Plate Fixation in Reverse Total Shoulder Arthroplasty," J. Shoulder Elbow Surg., **20**(3), pp. 467–476.
[3] Humphrey, C. S., Kelly, J. D., 2nd., and Norris, T. R., 2008, "Optimizing Glenosphere Position and Fixation in Reverse Shoulder Arthroplasty, Part Two: The Three-Column Concept," J. Shoulder Elbow Surg., **17**(4), pp. 595–601.
[4] James, J., Allison, M. A., Werner, F. W., McBride, D. E., Basu, N. N., Sutton, L. G., and Nanavati, V. N., 2013, "Reverse Shoulder Arthroplasty Glenoid Fixation: Is There a Benefit in Using Four Instead of Two Screws?," J. Shoulder Elbow Surg., **22**(8), pp. 1030–1036.
[5] Stephens, B. F., Hebert, C. T., Azar, F. M., Mihalko, W. M., and Throckmorton, T. W., 2015, "Optimal Baseplate Rotational Alignment for Locking-Screw Fixation in Reverse Total Shoulder Arthroplasty: A Three-Dimensional Computer-Aided Design Study," J. Shoulder Elbow Surg., **24**(9), pp. 1367–1371.
[6] Ackland, D. C., Patel, M., and Knox, D., 2015, "Prosthesis Design and Placement in Reverse Total Shoulder Arthroplasty," J. Orthop. Surg. Res., **10**(1), p. 101.
[7] Jarrett, C. D., Brown, B. T., and Schmidt, C. C., 2013, "Reverse Shoulder Arthroplasty," Orthop. Clin. North Am., **44**(3), pp. 389–408.
[8] Nam, D., Kepler, C. K., Neviaser, A. S., Jones, K. J., Wright, T. M., Craig, E. V., and Warren, R. F., 2010, "Reverse Total Shoulder Arthroplasty: Current Concepts, Results, and Component Wear Analysis," J. Bone Jt. Surg. Am., **92**(Suppl_2), pp. 23–35.
[9] Affonso, J., Nicholson, G. P., Frankle, M. A., Walch, G., Gerber, C., Garzon-Muvdi, J., and McFarland, E. G., 2012, "Complications of the Reverse Prosthesis: Prevention and Treatment," Instr. Course Lect., **61**, pp. 157–168.
[10] Stroud, N. J., DiPaola, M. J., Martin, B. L., Steiler, C. A., Flurin, P.-H., Wright, T. W., Zuckerman, J. D., and Roche, C. P., 2013, "Initial Glenoid Fixation Using Two Different Reverse Shoulder Designs With an Equivalent Center of Rotation in a Low-Density and High-Density Bone Substitute," J. Shoulder Elbow Surg., **22**(11), pp. 1573–1579.
[11] Zumstein, M. A., Pinedo, M., Old, J., and Boileau, P., 2011, "Problems, Complications, Reoperations, and Revisions in Reverse Total Shoulder Arthroplasty: A Systematic Review," J. Shoulder Elbow Surg., **20**(1), pp. 146–157.
[12] Critchley, O., McLean, A., Page, R., Taylor, F., Graves, S., Lorimer, M., Peng, Y., Hatton, A., and Bain, G., 2020, "Reverse Total Shoulder Arthroplasty Compared to Stemmed Hemiarthroplasty for Proximal Humeral Fractures: A Registry Analysis of 5946 Patients," J. Shoulder Elbow Surg., **29**(12), pp. 2538–2547.
[13] Hopkins, A. R., Hansen, U. N., Bull, A. M., Emery, R., and Amis, A. A., 2008, "Fixation of the Reversed Shoulder Prosthesis," J. Shoulder Elbow Surg., **17**(6), pp. 974–980.
[14] Pilliar, R. M., Lee, J. M., and Maniatopoulos, C., 1986, "Observations on the Effect of Movement on Bone Ingrowth Into Porous-Surfaced Implants," Clin. Orthop. Relat. Res., **208**, pp. 108–113.
[15] Szmukler-Moncler, S., Salama, H., Reingewirtz, Y., and Dubruille, J. H., 1998, "Timing of Loading and Effect of Micromotion on Bone-Dental Implant Interface: Review of Experimental Literature," J. Biomed. Mater. Res., **43**(2), pp. 192–203.
[16] Virani, N. A., Harman, M., Li, K., Levy, J., Pupello, D. R., and Frankle, M. A., 2008, "In Vitro and Finite Element Analysis of Glenoid Bone/Baseplate Interaction in the Reverse Shoulder Design," J. Shoulder Elbow Surg., **17**(3), pp. 509–521.
[17] Zhang, M., Junaid, S., Gregory, T., Hansen, U., and Cheng, C. K., 2019, "Effect of Baseplate Positioning on Fixation of Reverse Total Shoulder Arthroplasty," Clin. Biomech. (Bristol, Avon), **62**, pp. 15–22.
[18] Hast, M. W., Chin, M., Schmidt, E. C., and Kuntz, A. F., 2020, "Corrigendum to 'Central Screw Use Delays Implant Dislodgement in Osteopenic Bone but Not Synthetic Surrogates: A Comparison of Reverse Total Shoulder Models' [J. Biomech. 93 (2019) 11-17]," J. Biomech., **101**, p. 109628.
[19] Chae, S. W., Lee, H., Kim, S. M., Lee, J., Han, S. H., and Kim, S. Y., 2016, "Primary Stability of Inferior Tilt Fixation of the Glenoid Component in Reverse Total Shoulder Arthroplasty: A Finite Element Study," J. Orthop. Res., **34**(6), pp. 1061–1068.
[20] Zhang, M., Junaid, S., Gregory, T., Hansen, U., and Cheng, C. K., 2020, "Impact of Scapular Notching on Glenoid Fixation in Reverse Total Shoulder Arthroplasty: An In Vitro and Finite Element Study," J. Shoulder Elbow Surg., **29**(10), pp. 1981–1991.
[21] Abdic, S., Lockhart, J., Alnusif, N., Johnson, J. A., and Athwal, G. S., 2021, "Glenoid Baseplate Screw Fixation in Reverse Shoulder Arthroplasty: Does Locking Screw Position and Orientation Matter?," J. Shoulder Elbow Surg., **30**(5), pp. 1207–1213.
[22] Lung, T. S., Cruickshank, D., Grant, H. J., Rainbow, M. J., Bryant, T. J., and Bicknell, R. T., 2019, "Factors Contributing to Glenoid Baseplate Micromotion in Reverse Shoulder Arthroplasty: A Biomechanical Study," J. Shoulder Elbow Surg., **28**(4), pp. 648–653.
[23] Roche, C., DiGeorgio, C., Yegres, J., VanDeven, J., Stroud, N., Flurin, P.-H., Wright, T., Cheung, E., and Zuckerman, J. D., 2019, "Impact of Screw Length and Screw Quantity on Reverse Total Shoulder Arthroplasty Glenoid Fixation for 2 Different Sizes of Glenoid Baseplates," JSES Open Access, **3**(4), pp. 296–303.
[24] Harman, M., Frankle, M., Vasey, M., and Banks, S., 2005, "Initial Glenoid Component Fixation in 'Reverse' Total Shoulder Arthroplasty: A Biomechanical Evaluation," J. Shoulder Elbow Surg., **14**(1 Suppl S), pp. 162S–167S.
[25] Formaini, N. T., Everding, N. G., Levy, J. C., Santoni, B. G., Nayak, A. N., and Wilson, C., 2017, "Glenoid Baseplate Fixation Using Hybrid Configurations of Locked and Unlocked Peripheral Screws," J. Orthop. Traumatol., **18**(3), pp. 221–228.
[26] Codsi, M. J., and Iannotti, J. P., 2008, "The Effect of Screw Position on the Initial Fixation of a Reverse Total Shoulder Prosthesis in a Glenoid With a Cavitary Bone Defect," J. Shoulder Elbow Surg., **17**(3), pp. 479–486.
[27] Formaini, N. T., Everding, N. G., Levy, J. C., Santoni, B. G., Nayak, A. N., Wilson, C., and Cabezas, A. F., 2015, "The Effect of Glenoid Bone Loss on Reverse Shoulder Arthroplasty Baseplate Fixation," J. Shoulder Elbow Surg., **24**(11), pp. e312–e319.
[28] Gutierrez, S., Greiwe, R. M., Frankle, M. A., Siegal, S., and Lee, W. E., 3rd., 2007, "Biomechanical Comparison of Component Position and Hardware Failure in the Reverse Shoulder Prosthesis," J. Shoulder Elbow Surg., **16**(3), pp. S9–S12.
[29] Hoenig, M. P., Loeffler, B., Brown, S., Peindl, R., Fleischli, J., Connor, P., and D'Alessandro, D., 2010, "Reverse Glenoid Component Fixation: Is a Posterior Screw Necessary?," J. Shoulder Elbow Surg., **19**(4), pp. 544–549.
[30] Irlenbusch, U., and Kohut, G., 2015, "Evaluation of a New Baseplate in Reverse Total Shoulder Arthroplasty - Comparison of Biomechanical Testing of Stability With Roentgenological Follow Up Criteria," Orthop. Traumatol. Surg. Res., **101**(2), pp. 185–190.
[31] Maletsky, L. P., Sun, J., and Morton, N. A., 2007, "Accuracy of an Optical Active-Marker System to Track the Relative Motion of Rigid Bodies," J. Biomech., **40**(3), pp. 682–685.
[32] Favre, P., Perala, S., Vogel, P., Fucentese, S. F., Goff, J. R., Gerber, C., and Snedeker, J. G., 2011, "In Vitro Assessments of Reverse Glenoid Stability Using Displacement Gages Are Misleading - Recommendations for Accurate Measurements of Interface Micromotion," Clin. Biomech. (Bristol, Avon), **26**(9), pp. 917–922.
[33] Gopfert, B., Krol, Z., Freslier, M., and Krieg, A. H., 2011, "3D Video-Based Deformation Measurement of the Pelvis Bone Under Dynamic Cyclic Loading," Biomed. Eng. Online, **10**(1), p. 60.
[34] Schmidt, J. B., Berg, D. R., Ploeg, H.-L., and Ploeg, L., 2009, "Precision, Repeatability and Accuracy of Optotrak® Optical Motion Tracking Systems," Int. J. Exp. Comput. Biomech., **1**(1), p. 114.
[35] Langohr, G. D. G., 2015, *Fundamentals of the Biomechanical Characteristics Related to the Loading of Reverse Total Shoulder Arthroplasty Implants and the Development of a Wear Simulation Strategy*, Electronic Thesis and Dissertation Repository, 3436, Western University, London, ON, Canada.
[36] Kwon, Y. W., Forman, R. E., Walker, P. S., and Zuckerman, J. D., 2010, "Analysis of Reverse Total Shoulder Joint Forces and Glenoid Fixation," Bull. NYU Hosp. Jt. Dis., **68**(4), pp. 273–280.
[37] Anglin, C., Wyss, U. P., and Pichora, D. R., 2000, "Mechanical Testing of Shoulder Prostheses and Recommendations for Glenoid Design," J. Shoulder Elbow Surg., **9**(4), pp. 323–331.
[38] Bicknell, R. T., Liew, A. S., Danter, M. R., Patterson, S. D., King, G. J. W., Chess, D. G., and Johnson, J. A., 2003, "Does Keel Size, the Use of Screws, and the Use of Bone Cement Affect Fixation of a Metal Glenoid Implant?," J. Shoulder Elbow Surg., **12**(3), pp. 268–275.
[39] Collins, D., Tencer, A., Sidles, J., and Matsen, F., 3rd., 1992, "Edge Displacement and Deformation of Glenoid Components in Response to Eccentric Loading. The Effect of Preparation of the Glenoid Bone," J. Bone Jt. Surg. Am., **74**(4), pp. 501–507.
[40] Karduna, A. R., Williams, G. R., Iannotti, J. P., and Williams, J. L., 1998, "Total Shoulder Arthroplasty Biomechanics: A Study of the Forces and Strains at the Glenoid Component," J. Biomech. Eng., **120**(1), pp. 92–99.
[41] Sukjamsri, C., Geraldes, D. M., Gregory, T., Ahmed, F., Hollis, D., Schenk, S., Amis, A., Emery, R., and Hansen, U., 2015, "Digital Volume Correlation and micro-CT: An in-Vitro Technique for Measuring Full-Field Interface Micromotion Around Polyethylene Implants," J. Biomech., **48**(12), pp. 3447–3454.